

QUANTUM HALL FERROMAGNET IN A DOUBLE WELL WITH VANISHING g -FACTOR.

L. E. G. ARMAS

*Instituto de Física da Universidade de São Paulo, São Paulo, Brazil.
legarmas@gmail.com*

G. M. GUSEV

*Instituto de Física da Universidade de São Paulo, São Paulo, Brazil.
gusev@romeo.if.usp.br*

T. E. LAMAS

*Instituto de Física da Universidade de São Paulo, São Paulo, Brazil.
erikson@if.usp.br*

A. K. BAKAROV

*Institute of Semiconductor Physics, Novosibirsk 630090, Russia
bakarov@thermo.isp.nsc.ru*

J. C. PORTAL

*GHMFL-CNRS, BP-166, F-38042, Grenoble, Cedex 9, INSA-Toulouse, 31077, Cedex 4, and
Institut Universitaire de France, Toulouse, France.
portal@insa-toulouse.fr*

Received 27 July 2008

We have studied the quantum Hall effect in $\text{Al}_x\text{Ga}_{1-x}\text{As}$ -double well structure with vanishing g -factor. We determined the density-magnetic field $n_s - B$ diagrams for the longitudinal resistance R_{xx} . In spite of the fact that the $n_s - B$ diagram for conventional GaAs double wells shows a striking similarity with the theory, we observed the strong difference between these diagrams for double wells with vanishing g -factor. We argue that the electron-electron interaction is responsible for unusual behavior of the Landau levels in such a system.

Keywords: Quantum Hall effect; double quantum well.

1. Introduction

Double wells separated by a thin layer exhibits many exotic properties in a strong magnetic field due to the interplay between interlayer and intralayer exchange interaction, which is controlled by the ratio of the interlayer distance and the magnetic length.¹ From the Landau fan diagram for a two-subband system level (see Fig.1a)

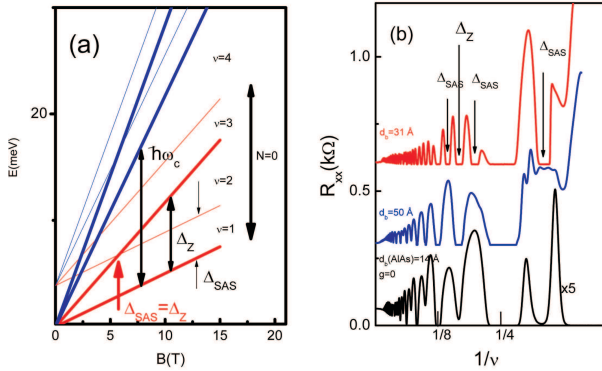


Fig. 1. (Color on line) (a) Energy diagram for a double well. (b) The longitudinal R_{xx} resistance for different DQW as a function of the inverse Landau filling factor (magnetic field). Minima with corresponding gaps are indicated. R_{xx} curves are shifted for clarity.

crossing at a total filling factor $\nu = 2$ is expected, because of the competition of the symmetric-antisymmetric Δ_{SAS} and Zeeman Δ_Z energies. As a result within the single particle picture a first order phase transition occurs at the $\Delta_{SAS} = \Delta_Z$ level crossing point, from a fully spin polarized ferromagnetic (F) state ($\Delta_Z > \Delta_{SAS}$) to a fully pseudospin polarized and spin paramagnetic single (S) state ($\Delta_{SAS} > \Delta_Z$). Within the many body picture the states F and S are strongly modified, for example, the F state consists of spin polarized states even in the limit of a vanishing g -factor, and the phase S state has an interlayer phase coherence for small layer separation, which exists in the limit of vanishing tunneling amplitude. Moreover, between F and S manybody phases, a novel canted (C) antiferromagnetic state has been predicted to emerge.² In this C state the average spin moment in the layers has an antiferromagnetic correlation in the plane perpendicular to the magnetic field, and a ferromagnetic correlation parallel to the magnetic field. The canted state exists for $\Delta_{SAS} > \Delta_Z$ and in the narrow interval of the layer separation. Systematic study of the phase diagram near the point $\Delta_{SAS} = \Delta_Z$ may give some experimental evidence for the existence of the canted phase in quantum Hall bilayer systems.

In the present paper we realized a new system $\text{Al}_x\text{Ga}_{1-x}\text{As}$ -double well structure with vanishing g -factor. The spin properties of the $\text{Al}_x\text{Ga}_{1-x}\text{As}$ quantum well depend strongly on the Al content x . For example, the effective g -factor changes with composition as $g_{\text{eff}}(x) = -0.44 + 2.7x$, therefore it is vanishing at $x \sim 10\%$. Since the F state is favored, when Δ_Z is increased, while the S state is favored, when Δ_{SAS} is increased, the canted phase is favored in the limit of vanishing g -factor and tunneling amplitude. We measured density-magnetic field phase diagrams and found level crossing at $\Delta_{SAS} = \Delta_Z$ at filling factor $\nu = 2$. We constructed the topological diagram in the density-magnetic field plane based on the single particle approximation. We found a striking similarity between experimental and theoretical diagrams for conventional double wells with $g=0.44$, and a strong difference between these diagrams for a double well with vanishing g -factor.

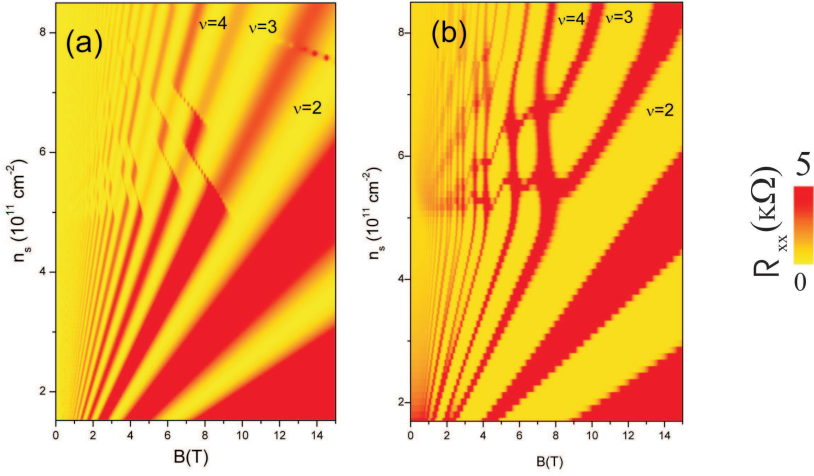


Fig. 2. (Color on line) Theoretical (a) and experimental (b) plots of the resistance in the density-magnetic field plane for double well structure with barrier thickness $d_b = 14 \text{ \AA}$ for tilt angle $\Theta=0$. Filling factors determined from Hall resistance are labeled. Filling factors $\nu = 4N + 1$ and $\nu = 4N + 3$ correspond to the tunneling gap.

2. Experimental Results and Discussion

The samples are symmetrically doped GaAs and $\text{Al}_{0.1}\text{Ga}_{0.9}\text{As}$ double quantum wells with equal widths $d_W = 140 \text{ \AA}$ separated by $\text{Al}_x\text{Ga}_{1-x}\text{As}$ and AlAs barriers with different width d_b varied from 14 to 31 \AA .³ The GaAs double well structures have a high total sheet electron density $n_s \approx 9 \times 10^{11} \text{ cm}^{-2}$ ($4.5 \times 10^{11} \text{ cm}^{-2}$ per one layer). The $\text{Al}_{0.1}\text{Ga}_{0.9}\text{As}$ double wells have a lower density $n_s \approx 6 \times 10^{11} \text{ cm}^{-2}$. Both layers are shunted by ohmic contacts. The relative densities in the wells are varied by the top gate which realized by a gold film. The voltage of the top gate raises or lowers only the density of the well which is closest to the sample surface (upper well), with the carrier density in the bottom well being almost constant. The Hall bars have a rectangular dimensions of $500 \times 200 \text{ \mu m}$. We measure both longitudinal and Hall resistances at temperatures $T = 50 \text{ mK}$ and in magnetic fields B up to 15 T using conventional ac-locking techniques with a bias current of 0.01-0.1 μA parallel to the layers. The mobility of the electrons in the GaAs double wells was $\mu \approx 10^6 \text{ cm}^2/\text{Vs}$ and in $\text{Al}_{0.1}\text{Ga}_{0.9}\text{As}$ double quantum wells $\mu \approx 0.7 \times 10^5 \text{ cm}^2/\text{Vs}$.

Fig. 1b shows typical traces for the longitudinal R_{xx} resistance for different DQWs as a function of inverse Landau level (LL) filling factor or perpendicular magnetic field. From the hierarchy of the energy gaps in a strong magnetic field (Fig. 1a) $\Delta_{SAS} < \Delta_Z < \hbar\omega_c$, where Δ_z is Zeeman splitting, $\omega_c = eB/mc$ is the cyclotron frequency, we identify the minima at $\nu = 4N$ with the cyclotron gap, minima at $\nu = 4N + 2$ with the Zeeman gap and minima at $\nu = 4N + 1(3)$ with the symmetric-asymmetric gap. It is obvious that the minima at $\nu = 4N$ are deepest, and one can identify 4-fold Landau level degeneracy. For the DQW with

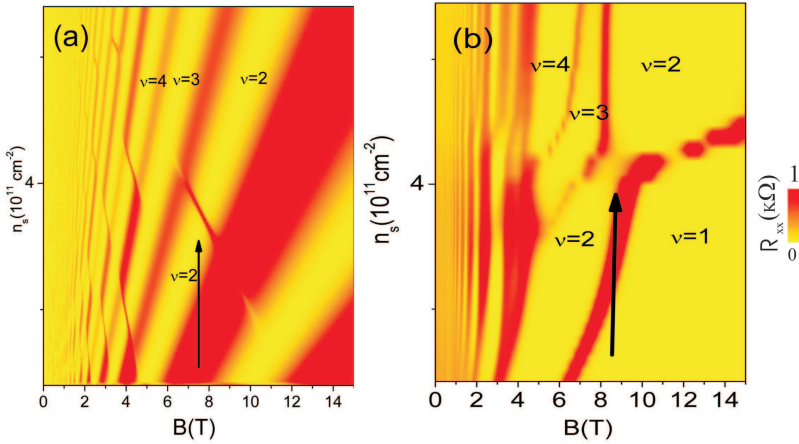


Fig. 3. (Color on line) Theoretical (a) and experimental (b) plot of the resistance in the density-magnetic field plane for $\text{Al}_{0.1}\text{Ga}_{0.9}\text{As}$ ($g=0$) double well structure with barrier (AlAs) thickness $d_b = 14 \text{ \AA}$ for tilt angle $\Theta=0$. Arrow shows the transition when $\Delta_{SAS} = \Delta_Z$.

the vanishing g -factor the gaps at $\nu = 4N + 2$ corresponding to the spin splitting are resolved due to quantum Hall ferromagnetism.

Surprisingly, we see deep minima at $\nu = 3$ which corresponds to Δ_{SAS} gap (see Fig. 1b). The symmetric-antisymmetric gap is calculated from a self consistent solution of the double well Schrödinger equation and Poisson's equation. According to our calculations this gap is 0.3 meV. It is smaller than the value extracted from low field double periodic Shubnikov de Haas oscillations (1.7 meV). However, we see no such splitting in a conventional DQW structure with $d_B = 50 \text{ \AA}$ and with much higher mobility ($\Delta_{SAS}=0.92 \text{ meV}$). Numerous scans of the resistance were taken at various V_g and the magnetic field sweepings. Figures 2 and 3 show the resulting phase diagrams, or the plots of the longitudinal resistance R_{xx} in $n_s - B_{\perp}$ plane for GaAs and $\text{Al}_{0.1}\text{Ga}_{0.9}\text{As}$ double wells. Such $n_s - B_{\perp}$ topological diagram, in general, corresponds to the energy LL fan diagram (Fig. 1a), however, several features are different. For example, in the level crossing regime we may see instead of the diamond-like structure, the so-called “ring-like” structure, which has been observed previously in square and parabolic wells with two occupied subbands.⁴⁻⁶ These features, in principle, can be explained in terms of the nonmonotonic behaviour of the Fermi energy at the Landau level crossing point within the single particle model.^{5,6} Fig. 2a shows such theoretical diagram calculated for a conventional GaAs double well structure. We can see the similarity between these two diagrams. From the position of the center of the rings we deduced the subband separation energy as a function the total electron density. Note that the Zeeman energy Δ_Z is given by $\Delta_{spin} = g^* \mu_B B = g_0 \mu_B B + E_{ex}$, where μ_B is the Bohr magneton, g_0 is bare Landé factor, $E_{ex} = \alpha \hbar \omega_c$, $\omega_c = eB/mc$ is the cyclotron frequency, m is the effective mass, $\alpha = (1/\pi k_{FA_B}) \ln(2k_{FA_B})$, k_F is the Fermi vector, a_B is Bohr radius. From this

equation we may see, that spin splitting appears in the limit of a vanishing bare g -factor, when the exchange energy is comparable with disorder broadening of the Landau levels. From the comparison of the size of the ring we extract the correlation energy E_{ex} and the coefficient α , which roughly agrees with a value $\alpha \sim 0.2$ determined for two subbands in square and parabolic wells.⁶

Figure 3 shows theoretical and experimental diagrams for $\text{Al}_{0.1}\text{Ga}_{0.9}\text{As}$ double quantum wells. Note the difference from the conventional GaAs double well. First, the “ring-like” structure is not resolved in $g=0$ samples due to the lower mobility. Second, we clearly see $\Delta_{SAS} = \Delta_Z$ level crossing point, indicated by arrows. Finally, we did not see similarity between theoretical and experimental diagrams, in contrast to the conventional GaAs double well structures (Fig. 2). For example, the magnetoresistance maxima after the crossing point at $\nu = 2$ deviate from the straight lines, which are expected for single-picture LL behaviour. We have performed numerical calculations for different adjustable parameters α and energy level separations, however, we found that the noninteracting model can not describe all topological features, particularly the collapse of the $\nu = 3$ and $\nu = 5$ minima at higher densities and the increasing of the $\nu = 2$ minima. It may indicate, that the canted state emerges at $\nu = 2$ when $\Delta_{SAS} > \Delta_Z$ and is responsible for structures in the $n_s - B$ topological diagram.

Acknowledgments

Support of this work by FAPESP, CNPq (Brazilian agencies) is acknowledged.

References

1. *Perspectives in quantum Hall effects*, edited by S. Das Sarma, and A. Pinzuk (John Wiley and Sons, New York, 1997).
2. S. Das Sarma, S. Sachdev, L. Zheng, *Phys.Rev.Lett.* **58**, 4672 (1998).
3. N. C. Mamani, G. M. Gusev, T. E. Lamas, A. K. Bakarov, O. E. Raichev, *Phys. Rev. B* **77**, 205327 (2008).
4. X. C. Zhang, D. R. Faulhaber, H. W. Jiang, *Phys.Rev.Lett.* **95**, 216801 (2005).
5. C. Ellenberger, B. Simovič, R. Letureq, T. Ihn, S. E. Ulloa, K. Ensslin, D. C. Driscoll, A. C. Gossard, *Phys.Rev. B* **74**, 195313 (2006).
6. C. A. Duarte, G. M. Gusev, A. A. Quivy, T. E. Lamas, A. K. Bakarov, J. C. Portal, *Phys. Rev. B* **76**, 075346 (2007).